



Seasonal variation in satellite-derived effects of aerosols on clouds in the Arabian Sea

Thomas A. Jones¹ and Sundar A. Christopher¹

Received 2 July 2007; revised 28 November 2007; accepted 30 January 2008; published 15 May 2008.

[1] Aerosols act as cloud condensation nuclei for cloud water droplets, with changes in aerosol concentrations having significant impacts on the corresponding cloud properties. An increase in aerosol concentration may lead to an increase in CCN, with an associated decrease in cloud droplet size for a given cloud liquid water content. Smaller droplet sizes may then lead to a reduction in precipitation efficiency and an increase in cloud lifetimes. However, these effects are highly dependent on the aerosol concentration, aerosol species, and the meteorological conditions. In the Arabian Sea (10–20°N, 62–72°E), prevailing aerosol type transitions from mostly small-mode anthropogenic aerosols during the winter months to mostly coarse-mode mineral dust and sea salt during the summer due to a change in prevailing wind speed and direction, is likely to impart substantial variability on any associated indirect effects. To examine this variability, we use one year (2004) of MODIS derived aerosol optical thickness (AOT) and cloud products over the Arabian Sea to quantify aerosol indirect effects. Results show that indirect effects in the Arabian Sea are a strong function of season, which is a result of the changing aerosol and moisture (humidity) concentrations during the course of the year. During the winter months (DJF), cloud-droplet size and AOT were found to have a weak positive correlation ($r = 0.12$), opposite of the expected effect. The low atmospheric humidity coupled with wide-spread subsidence and other dynamical factors may prevent these aerosols from being activated. During the summer months (JJA), AOT increases with the addition of mineral dust and sea salt aerosols and the correlation between AOT and cloud droplet size becomes negative ($r = -0.22$). The magnitude of the first indirect effect corresponds to an increase in low level wind speeds, increasing the concentration of hygroscopic sea salt into the atmosphere. For both periods, a positive correlation ($r = 0.16, 0.32$) was found between AOT and LWP indicating a reduction in precipitation efficiency.

Citation: Jones, T. A., and S. A. Christopher (2008), Seasonal variation in satellite-derived effects of aerosols on clouds in the Arabian Sea, *J. Geophys. Res.*, 113, D09207, doi:10.1029/2007JD009118.

1. Introduction

[2] The introduction of large amounts of carbonates and sulfates from anthropogenic sources into the atmosphere has led to a substantial increase in atmospheric aerosol concentrations over certain regions of the planet. Since aerosols often reflect incoming solar radiation back into space, increasing AOT leads to a cooling of the atmosphere, which is known as the direct effect [e.g., Christopher and Zhang, 2004]. Small-mode ($r_e < 0.25 \mu\text{m}$) and sulfate based aerosols (where r_e is the effective radius of an aerosol particle) often act as cloud condensation nuclei (CCN) for warm-process clouds [e.g., Quaas *et al.*, 2004; Lohmann and Feichter, 2005; Penner *et al.*, 2004]. Both observations and modeling studies have shown that as anthropogenic aerosol concentration increases, the number of CCN in-

crease accordingly, leading to a decrease in water cloud droplet size assuming a constant liquid water path through the cloud [e.g., Jones *et al.*, 1994]. This is known as the first indirect, or the Twomey effect [Twomey, 1977; Kaufman and Fraser, 1997; Feingold, 2003]. The decrease in droplet size has the additional effect of delaying the onset of collision and coalescence in maritime stratocumulus clouds, reducing precipitation efficiency and increasing the lifespan and possibly the areal coverage of the cloud, which is labeled as the second indirect effect [Albrecht, 1989; Quaas *et al.*, 2004]. Reducing precipitation efficiency also acts to increase water loading, leading to an increase in cloud liquid water path (LWP) and a corresponding increase in cloud thickness, complicating the identification of the Twomey effect in observations [Han *et al.*, 1998; Reid *et al.*, 1999; Schwartz *et al.*, 2002]. Given the complex interaction between aerosols and warm cloud characteristics, it is likely that they differ significantly as a function of space and time due to changing meteorological and aerosol-type properties [Matsui *et al.*, 2006]. A comprehen-

¹Department of Atmospheric Science, The University of Alabama in Huntsville, Huntsville, Alabama, USA.

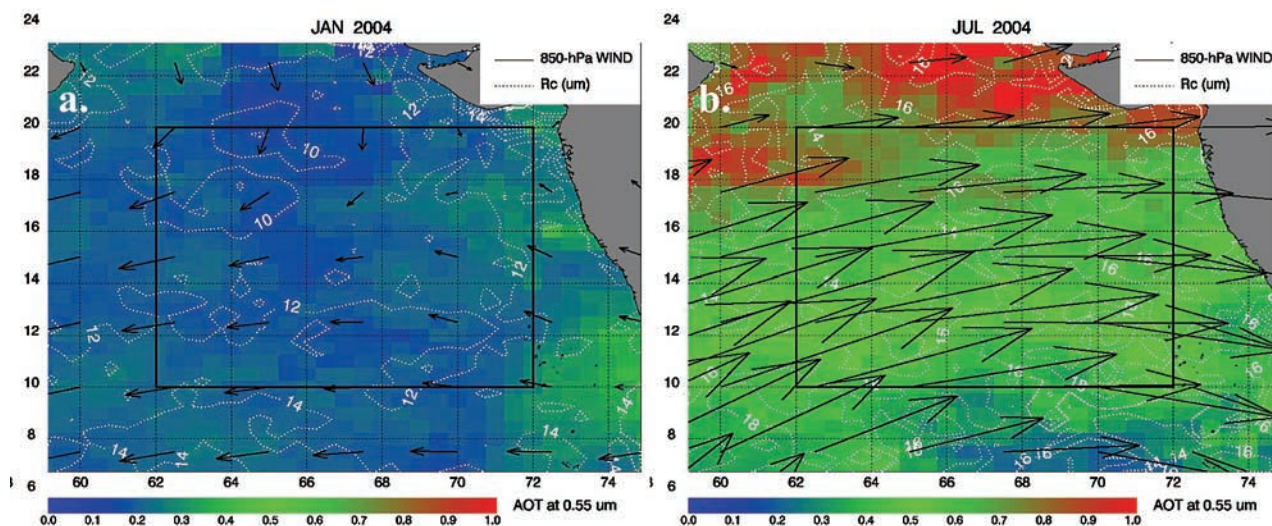


Figure 1. Spatial distribution of MODIS AOT at $0.55 \mu\text{m}$ and cloud droplet effect radius (R_c) during January (a) and July (b) 2004. NCEP derived 850 hPa wind vectors are over-plotted to indicate aerosol source regions for each month. The box indicates the region from which statistics are generated.

sive review of aerosol indirect effects is given by *Lohmann and Feichter [2005]*.

[3] Traditionally small-mode, hygroscopic aerosols (e.g., sulfates produced from anthropogenic sources) are considered the most efficient CCN beyond naturally occurring sea salt in highly polluted regions such as the northern Indian Ocean [*Jones et al., 1994; Li et al., 1996*]. Over the ocean, aerosol indirect effects are generally prevalent near locations where anthropogenic sulfates are produced, such as ship tracks and downwind of major pollution sources [*Ackerman et al., 2003; Avey et al., 2007; Bennartz, 2007*]. Since the background aerosol concentration is low, the indirect effect caused by the addition of large concentrations of anthropogenic aerosols is most noticeable over the ocean [*Han et al., 1998; Lohmann and Lesins, 2003*]. The influence of additional aerosol types, such as dust, on CCN and cloud characteristics has been less well documented. However, non-hygroscopic mineral dust can act as large CCN when coated with soluble material such as sulfate [*Levin et al., 1996*].

[4] One area where substantial concentrations of clouds and aerosols, depicted when cloud and aerosol optical thickness are large, exist is the Arabian Sea, west of the Indian subcontinent [*Ramanathan et al., 2007*]. Anthropogenic aerosols transported over the ocean from India account for the greatest proportion of total aerosol concentration during the winter months, while dust aerosols transported from the Arabian Peninsula in concert with increased sea-salt produced from higher wind speeds are predominant during the summer months [*Ramanathan et al., 2001; Ramana and Ramanathan, 2006*]. Using 5 years of January data, *Chylek et al. [2006]* observed that cloud droplet radius decreases from south to north in the Indian Ocean (15°S to 25°N) due to a corresponding increase in anthropogenic aerosol concentration. They considered the month of September as a “clean” case for comparison, despite the presence of large concentrations of dust and sea salt aerosols in the Arabian Sea, which were not accounted for in their analysis.

[5] Previous studies have often focused on analyzing the indirect effect on very small temporal and spatial scales [e.g., *Reid et al., 1999*] or on a globally averaged scale [e.g., *Matsui et al., 2006*] often without comparing the effect due to changes in aerosol properties. In both cases, the indirect effects due to changes in aerosol type and meteorology over long periods of time on a regional scale are generally overlooked. To analyze the effect of aerosols and aerosol type on cloud coverage as a function of time, we use aerosol and cloud data from the Moderate Resolution Imaging Spectroradiometer (MODIS) instrument onboard the Terra spacecraft for a one year period (December 2003–November 2004). We selected a 10×10 degree region in the Arabian Sea ($62\text{--}72^\circ\text{E}$, $10\text{--}20^\circ\text{N}$) for study that contains a multitude of aerosol types (e.g., sea salt, dust, sulfates, black and organic carbon) for this research. This region was chosen due to its distinct seasonal cycle in winds, cloud coverage, and aerosol properties. The goal of this research is to analyze the changes in cloud properties on a seasonal timescale as a function of changes in aerosol properties and meteorology from a satellite perspective.

2. Data

2.1. Cloud Properties

[6] Clouds and Earth’s Radiant Energy System (CERES) Single Scanner Footprint (SSF) FM1, Edition 2B data between December 2003 and November 2004 from the Terra satellite were collected for a 10×10 degree region over the Arabian Sea (Figure 1). The CERES-SSF product combines the radiative fluxes retrieved from the CERES instrument with aerosol properties from the MOD04 (Collection 4) product and cloud properties retrieved from MODIS [*Remer and Kaufman, 2005; Minnis et al., 2003*]. At nadir, CERES-SSF footprint resolution is ~ 20 km with a near daily global coverage. Cloud properties include cloud liquid water path (LWP), cloud water effective droplet radii (R_c), cloud optical thickness (COT), and cloud top pressure (CTP) retrieved from the $3.7 \mu\text{m}$ (near-infrared) channel

[Minnis *et al.*, 2003]. For adiabatically stratified water clouds, the theoretical relationship between R_c and LWP is described by equation (1) where ρ is the density of liquid water and τ_c is cloud layer optical depth [e.g., Wood and Hartmann, 2006].

$$LWP = \frac{5}{9} \rho \tau_c R_c \quad (1)$$

[7] The MODIS is capable of resolving cloud characteristics at 2 different levels, one nearer to the surface, the other (if it exists) higher in the atmosphere. However, the primary focus of this study is warm process water clouds, so only data from the lower cloud layer are considered. The MODIS algorithm uses visible wavelengths to retrieve cloud optical depth and near IR to mid-IR measurements to retrieve cloud droplet size that are then converted to LWP using equation (1) [e.g., Greenwald and Christopher, 2000]. The only constraint placed on the data (outside normal quality control flags) is that MODIS cloud data are only used when the MODIS cloud phase parameter indicates that the cloud in question is at least 95% composed of liquid water droplets. The effects of aerosols on ice clouds are beyond the scope of this study. We use the cloud property retrievals in the CERES-SSF product since it contains broadband top of atmosphere shortwave and longwave fluxes that is being used in ongoing research to determine the regional variations in combined aerosol-cloud climate effects. Compared to the cloud retrieval in the MOD06 product, CERES-SSF generally produces smaller cloud droplet size and cloud optical thickness values, though the overall patterns are generally the same with overall cloud amounts differing less than 10% [Minnis *et al.*, 2003]. Han *et al.* [1994] provide a review of the various error sources in the retrieval process including calibration, assumptions in atmospheric and surface properties, ambiguous solutions for optically thin clouds calibration, vertical inhomogeneity of clouds and cirrus contamination. The most significant uncertainty related to this research is the uncertainty associated with optically thin clouds [e.g., Nakajima and King, 1990]. Under these circumstances, the relationship between retrieved cloud optical thickness and cloud droplet effective radius may break down. However, we cannot ignore optically thin cloud as part of this research as they contribute a large portion of the total cloud cover, especially during the winter months. Since we are focusing on the change in cloud characteristics due to aerosols, a bias one way or the other should not significantly affect the outcome of this research. Also, we derive relationships as a function of different cloud thicknesses, noting any differences that may exist from thin to thick clouds.

2.2. Aerosol Properties

[8] Cloud properties are combined with MODIS derived aerosol optical thickness (AOT) and fine mode fraction (FMF) at $0.55 \mu\text{m}$. MODIS AOT is derived from clear-sky 500 m pixels and aggregated to 10 km footprint used by the MODIS level 2 aerosol product (MOD04). Assuming some number of clear-sky pixels exist within each 10 km footprint, a total and small-mode AOT value for that footprint is reported along with the fraction of that 10 km footprint covered by clouds. The cloud fraction product in

the MOD04 product ranges from 0 (indicating completely clear) to 1.0, indicating totally cloudy scenes. Aerosol retrievals are often possible for cloud fractions up to 0.95. MODIS resolution AOT is then converted to CERES resolution product using a point spread weighting function. CERES resolution AOT will exist unless nearly 100% cloud cover exists over an entire CERES footprint, which occurs <10% of the time.

[9] FMF fraction is a measure of aerosol size with large values of FMF indicating *mostly* small-mode (e.g., largely anthropogenic) aerosols present, with low values indicating *mostly* coarse-mode (e.g., coarse sea salt and/or mineral dust) present [Kaufman *et al.*, 2005]. We use FMF as a tool to determine the effect of aerosol type on cloud characteristics. Previous research indicates that the Twomey effect should be greatest in the presence of small-mode aerosols in relatively moist environments [e.g., Heintzenberg *et al.*, 1997; Quaas *et al.*, 2004]. While this is certainly the case in certain circumstances, the complexities of the aerosol-cloud droplet interaction mean that no one process can often be singled out. AOT, FMF, R_c , and LWP will be compared to determine the nature and changes of the indirect effects in the Arabian Sea as a function of time.

2.3. Goddard Chemistry Aerosol Radiation Transport (GOCART)

[10] The satellite-derived AOT properties are compared with AOT simulations produced by the GOCART model [Chin *et al.*, 2004]. GOCART simulates the transport of aerosols and their species over a global domain. Aerosols are categorized as black and organic carbon, sulfate, dust, and maritime sea salt. The naturally occurring portions of organic carbon and sulfate (DMS) are also reported separately from the total organic carbon and sulfate concentrations. Monthly averaged data on a 2.5×2 degree grid were acquired for each region between December 2003 and November 2004. Total AOT from GOCART is the sum of the optical depth from each component aerosol listed above over the entire atmospheric column. Chin [2002] and Chin *et al.* [2004] provide a thorough description of the differences between the MODIS and GOCART. GOCART uses global emissions of aerosols and assimilated meteorological fields to calculate the mass loading of each aerosol species separately that are then converted to AOT using mass extinction coefficients. GOCART model output is used to determine the concentrations of various aerosol species in the Arabian Sea on a monthly basis.

2.4. Meteorology

[11] Monthly mean, global surface wind speed and direction, and relative humidity at 1000, 850, and 700 hPa levels were obtained from National Centers for Environmental Prediction (NCEP) Reanalysis data. The NCEP Reanalysis contains global meteorological conditions with a 2.5 degree horizontal resolution and a 17 level vertical resolution at 6 h time intervals [Kalnay *et al.*, 1996]. The reanalysis data set reliability captures synoptic scale dynamic and thermodynamic features, though often misses smaller scale phenomena. Total column humidity is included within the CERES-SSF product co-located with the CERES footprint and is derived by averaging relative humidity (RH) observations at all levels taken from ECMWF model analysis.

Total column humidity is used to bin aerosol and cloud data when studying the second indirect effect.

3. Results and Discussion

3.1. Aerosol Overview

[12] MODIS AOT in the Arabian Sea increases substantially between April and May 2004 before decreasing just as substantially by September (Figure 2a). For the same time

period, modeled GOCART AOT shows a similar trend (Figure 2b). The increase in AOT between April and May and into June is largely due to a ~50% increase in dust (coarse-mode) aerosol concentration, which has the effect of lowering MODIS FMF by ~25% at the same time (Figures 2a and 2b). The dust component of AOT remains high into August with a value of 0.11 or 40% of the total AOT, with an increase in the maritime (sea salt) component of AOT also occurring between June and August. Between April and August, dust aerosols are transported into the Arabian Sea from the deserts over the Arabian Peninsula by increasing west winds associated with the onset of the Indian Monsoon [Ramana and Ramanathan, 2006]. Near surface (1000 hPa) wind speeds associated with the Monsoon are greatest between June and August ($>10 \text{ ms}^{-1}$), directly corresponding to the increase in maritime sea salt during this time [Colón-Robles et al., 2006]. As a result, the decrease in MODIS FMF during the summer months is likely a combination of dust and sea salt aerosols, neither of which is present in large concentrations during the winter (Figure 2b). Total column, 850 and 700 hPa relative humidity as well as MODIS cloud fraction are greatest between June and September corresponding to increasing cloud cover associated with the Monsoon (Figure 2c). Near surface humidity is much less variable due to its proximity to the ocean surface.

[13] In the winter, the primary contributor to total AOT is sulfates (according to GOCART) transported from the Indian subcontinent into the Arabian Sea (Figures 1a and 2b). The high proportion of anthropogenic aerosols during in winter is consistent with the high (>0.65) FMF values observed by MODIS (Figure 2a). GOCART indicates that sulfate aerosols remain in the atmosphere throughout the entire year period, despite the influx of additional aerosol types. The contribution from black and organic carbon is quite small accounting for less than 5% of the total AOT for all months (Figure 2b). Also, DMS only accounts for approximately 10% of the total sulfate concentration throughout the year (not shown). The increase in dust and sea salt aerosols during the summer months, which more than doubles the AOT, directly influences the relationship between AOT, R_c , and LWP. Two months, January and July, are examined in detail below to analyze the differences in indirect effect as a function of changes between winter and summer aerosol and atmospheric conditions in the Arabian Sea. Changes in these parameters are important, since previous observations of the aerosol indirect effects have noted that they are most significant for thick clouds in high

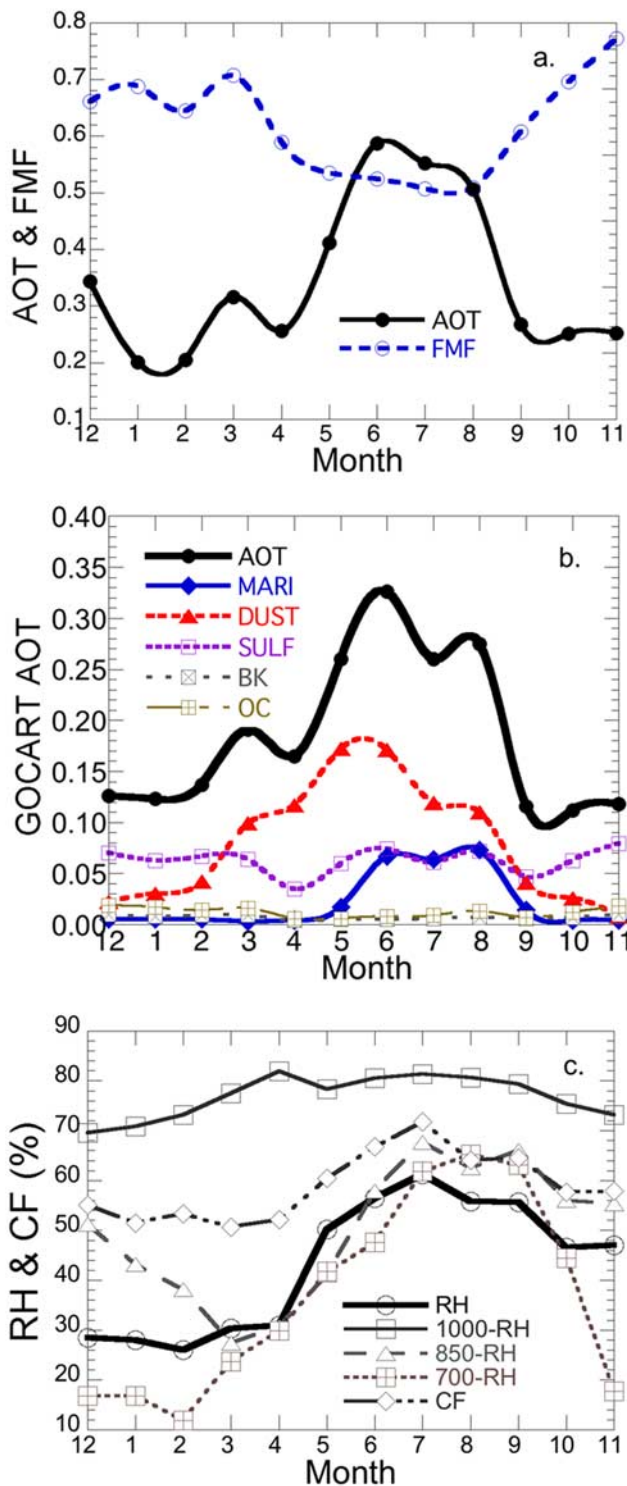


Figure 2. Time series of MODIS AOT and FMF at $0.55 \mu\text{m}$ for the Terra overpass time averaged from raw data over the entire area for each one month period (a). GOCART generated aerosol optical thickness components between December 2003 and November 2004 (b). Aerosol components shown include, maritime sea salt (MARI), mineral dust (DUST), total sulfate (SULF), black carbon (BK), and organic carbon (OC), with total GOCART AOT also plotted. NCEP relative humidity at 1000, 850, and 700 hPa, total column humidity (RH) from the ECMWF, and MODIS cloud fraction (CF) from Terra (c).

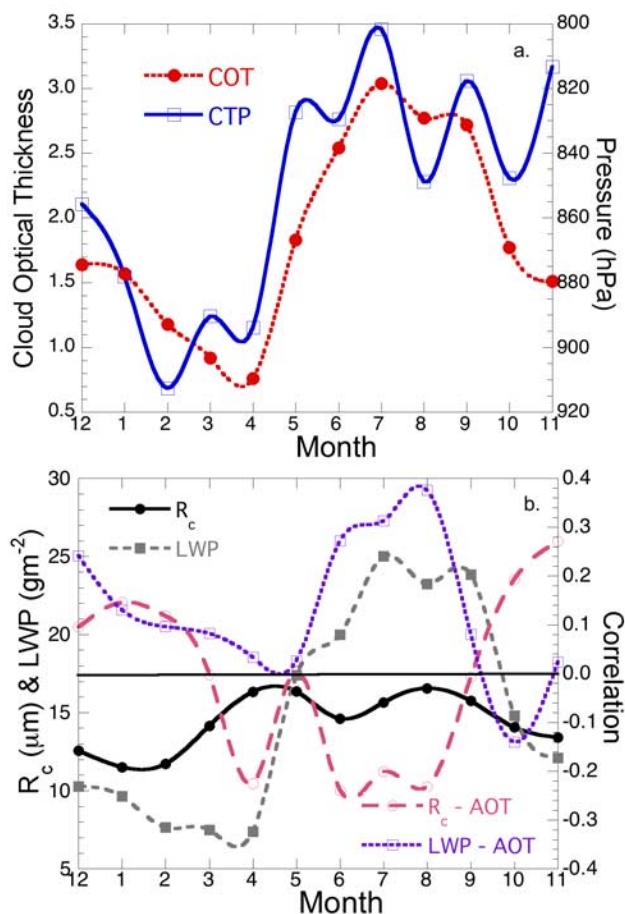


Figure 3. Time series of MODIS cloud optical thickness and cloud top pressure (a). Correlation between MODIS cloud liquid water droplet effective radius (R_c) and cloud liquid water path (LWP) and AOT in the Arabian Sea between December 2003 and November 2004 (b).

moisture conditions, which are more prevalent during the summer months [e.g., Lohmann *et al.*, 2000].

3.2. Winter

[14] Between January and April, the primary aerosol species in the Arabian Sea consists of those produced from anthropogenic pollution containing a high proportion of sulfates that originate from the Indian sub-continent [Ramana and Ramanathan, 2006; Quinn *et al.*, 2002]. This is also evident from available GOCART model (Figure 2b). Small contributions from dust and organic carbon account for most of the remainder of total AOT. Sulfates are hygroscopic and will act as excellent CCN in the presence of adequate atmospheric moisture. However, atmospheric humidity is quite low, with total column humidity less than 30% (Figure 2c). Much of the moisture present is concentrated near the surface, with moisture availability decreasing rapidly with heights (700 hPa RH < 20%). The mean 850 hPa vertical velocity of 0.04 Pa s^{-1} indicates subsidence, which can also reduce boundary layer height. Combined, these conditions act to suppress cloud formation leading to optically thin clouds. (CTP \sim 890 hPa,

COT < 2.0, Figure 3a). Similar, low-thin cloud properties were observed during the INDOEX project between January and March 1999 [Ramanathan *et al.*, 2001]. In these conditions, the indirect effect is not well understood and satellite based observations may have larger uncertainties [Lohmann *et al.*, 2000]. The resulting relationship between AOT and cloud droplet size is *positive*, with a correlation coefficient of 0.13 (Figure 3b). The corresponding winter season (DJF) correlation is similar (0.12). All correlation statistics are calculated using daily swath-level data during a particular 1 month period with no spatial or temporal averaging. Also, data are not binned prior to the calculation of the correlation statistics provided in Figure 3b.

[15] Figure 4a shows effective radius as a function of AOT, with data binned in 5 gm^{-2} LWP intervals to examine the effect of cloud thickness on the first indirect effect [e.g., Feingold *et al.*, 2003]. (The sample size within each AOT bin is maximized for the AOT bin just less than the mean January AOT, with the variability in sample size per bin rarely exceeding one order of magnitude. This indicates that no significant sampling biases are being introduced during the plotting process). In January, cloud thickness is not a significant factor in the AOT- R_c relationship, though most of the data have LWP values less than 20 gm^{-2} . Correlation statistics computed for LWP < 20 gm^{-2} and LWP > 20 gm^{-2} , are not significantly different, both being weakly positive. Spatial correlation between monthly averaged AOT and R_c was also low (Figure 1a). While these observations are not indicative of the presence of the first indirect effect, they are consistent with observations that more polluted air is often associated with drier, thinner clouds, due to the continental origin of the air mass [Brenguier *et al.*, 2003]. Under these conditions, a positive relationship between AOT and droplet size has been observed [Peng *et al.*, 2002; Yuan *et al.*, 2007]. It is also possible that the small, but non-zero, presence of absorbing BC aerosols leads to warming of the atmosphere, increasing stability, and reducing cloud cover through evaporation [Ackerman *et al.*, 2003; Lohmann and Feichter, 2005]. However, this process would also lead to an inverse relationship between AOT and LWP, which is not observed here.

[16] Of interest is the relationship between cloud droplet size and FMF (Figure 4b) in which cloud droplet size decreases by almost 50% when FMF is greater than 0.8 and LWP is less than 10 gm^{-2} . FMF values greater than 0.8 indicate that the aerosols are primarily small-mode and likely anthropogenic in nature [Bellouin *et al.*, 2005; Kaufman *et al.*, 2005]. This feature was observed during other winter months (not shown). These aerosols are likely associated with the “anthropogenic haze” noted by Ramanathan *et al.* [2001], which was observed over the northern Indian Ocean during the winter months of 1999 as part of the INDOEX project. With the exception of aerosols with a FMF > 0.8, little evidence of the first indirect effect is present in January in the Arabian Sea. However, evidence for the second indirect effect, the reduction of precipitation efficiency, does exist. Here, we use changes in cloud thickness as a function of AOT as an indicator of changes in precipitation efficiency [Albrecht, 1989]. Figure 5a shows a positive relationship between AOT and LWP, binned into 10% total column relative humidity bins. The correlation

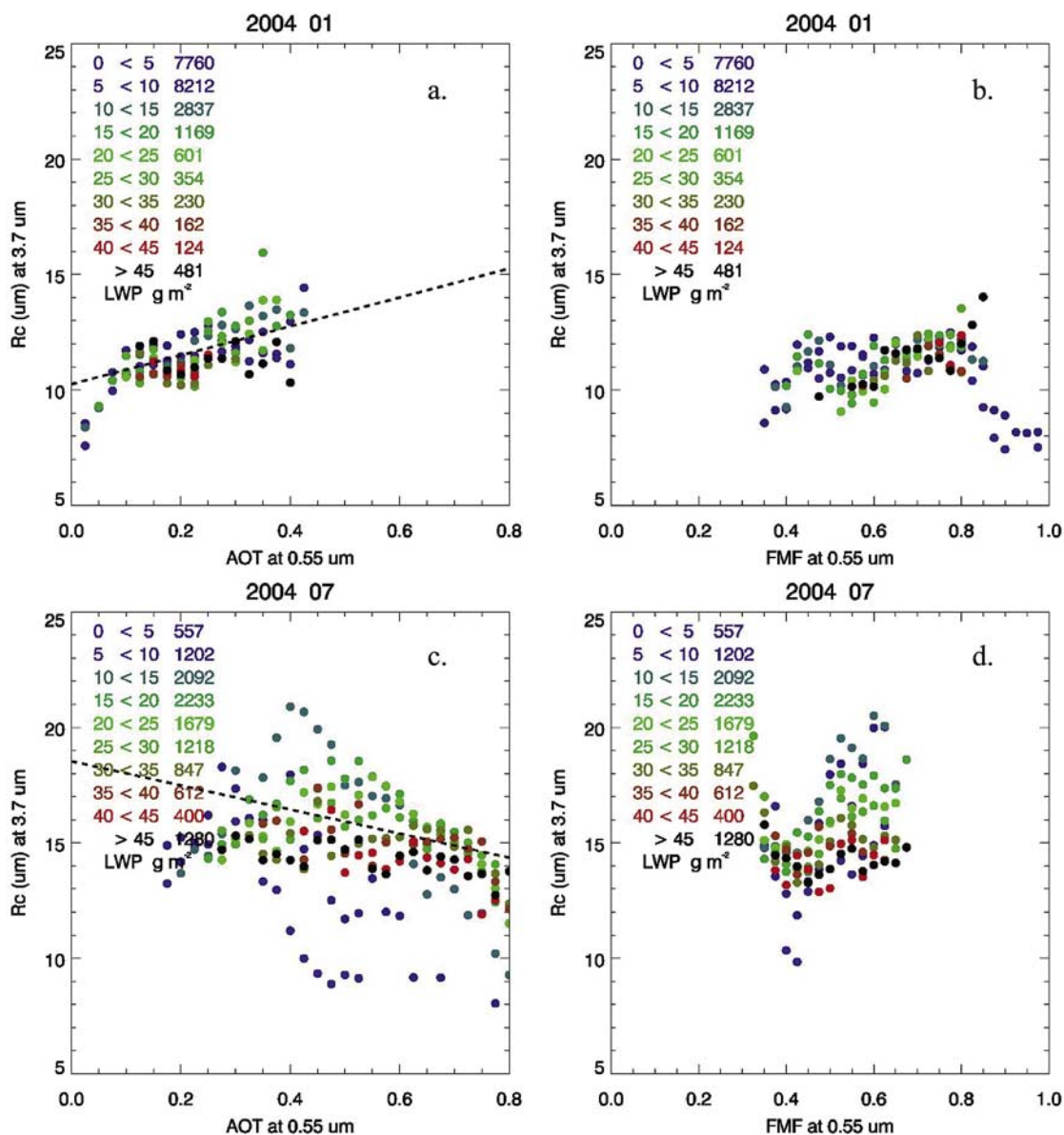


Figure 4. Scatterplot of MODIS AOT and FMF versus cloud droplet effective radius for January (a,b) and July (c,d) 2004. Data are grouped into 5 g m^{-2} LWP bins, with sample size for each bin listed, to indicate the effect of cloud thickness on the first indirect effect. Linear regression fits are plotted for AOT- R_c relationships.

coefficient is 0.13 for all RH bins, and is positive for RH bins greater than 10% with correlation coefficient increasing as a function of RH. Also note that total column relative humidity never exceeds 60%, corresponding to the low cloud fraction and thin clouds present at this time. Still, the increase in LWP as a function of AOT indicates that aerosols may be reducing precipitation efficiency, allowing the moisture content of the clouds to increase which is consistent with observations by *Albrecht* [1989]. Unfortunately, it has proven difficult to discriminate aerosol from non-aerosol influenced precipitation from observations, which would be the most direct measurement of the second indirect effect. The question as to why this effect was observed while the first indirect effect was not remains unclear and requires further investigation.

[17] LWP was also calculated using MODIS cloud optical depth and effective radius using equation (1), and plotted in Figure 5a showing an excellent correspondence between the algorithm-derived and expected LWP values, illustrating the consistency of the retrieval algorithm for various cloud properties. Equation (1) also indicates that LWP should be a linear function of R_c for a given cloud optical thickness. Figure 4b shows that this is indeed the case, but also shows that the slope of the LWP- R_c relationship increases for thicker clouds, consistent with observations by *Nakajima et al.* [1991] and *Han et al.* [1994] for $\text{COT} < 15$.

3.3. Summer

[18] Between April and May, relative humidity and total AOT increase, both in response to the onset of the Indian

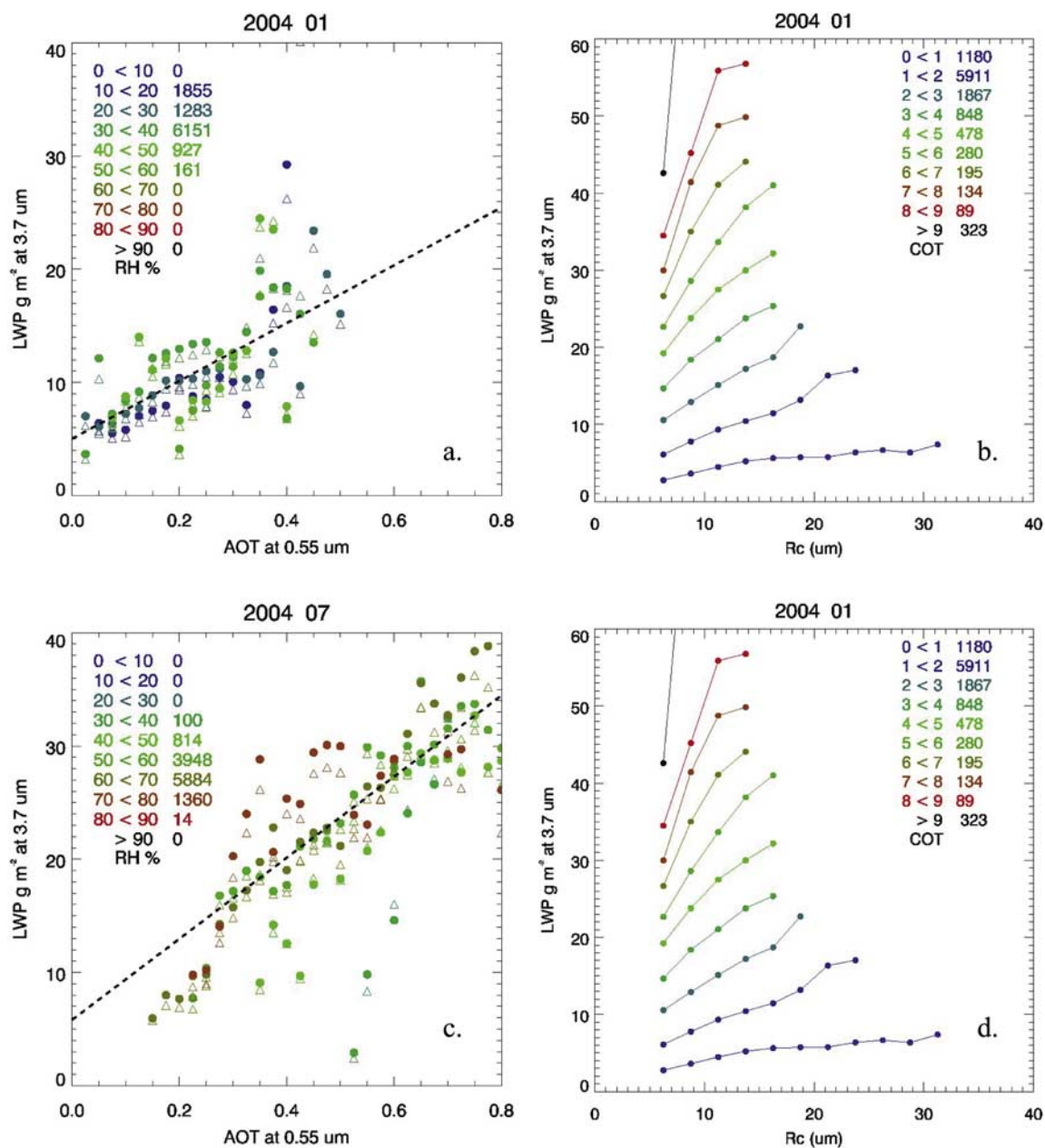


Figure 5. MODIS LWP plotted as a function of AOT (filled dots), this time grouped into 10% RH bins, showing the presence of the second indirect effect for January (a) and July (c) 2004, with linear regression fits over plotted. LWP values derived from equation (1) are plotted for comparison (open triangles). For the same months, LWP as a function of cloud droplet effective radius (R_c) binned by cloud optical thickness are also shown (b, d).

monsoon (Figure 2). Average cloud droplet size also increases in response to the greater amount of moisture and synoptic forcing available for droplet formation. Evidence for greater average synoptic forcing exists in the NCEP vertical velocity at 850 hPa. In July an average upward velocity of -0.05 Pa s^{-1} was observed compared to subsidence of 0.04 Pa s^{-1} recorded during January, which would also increase the likelihood of deeper (higher COT, LWP) clouds during this month. The increase in AOT is the result of the addition of large amounts of dust aerosols to the

region and increased sea salt production from monsoon enhanced wind speeds, both evident in Figure 1b. The influx of coarse-mode sea salt and dust aerosols also lowers overall FMF compared to other months (Figures 2a and 2b). Unlike the winter months described above, a negative correlation between AOT and cloud droplet size does exist between the months of June and August, when total AOT is maximized, indicating the presence of the first indirect effect (Figure 3b). The inverse relationship between AOT and cloud droplets during July is most evident when

MODIS AOT is greater than 0.4, with the correlation maximized when LWP is less than 30 gm^{-2} (Figure 4c). June and August show similar results with an overall summer season (JJA) correlation coefficient of -0.22 . (A negative correlation was also observed during the month of April prior to the increase in AOT and atmospheric humidity, but the reasons for this apparent outlier remain unclear).

[19] This is in stark contrast to January, when a positive relationship between AOT and cloud droplet size was observed. However, note that the maximum AOT in January barely exceeds 0.4, the threshold where the first indirect effect relationship becomes most evident during the summer. This threshold is similar to that found by *Brennan et al.* [2006] above which the MOD06 cloud algorithm incorrectly classifies large concentrations of dust aerosols as clouds, resulting in an underestimation of overall cloud-droplet radius. However, we are not using the MOD06 product, but rather the one described by *Minnis et al.* [2003]. We carefully analyzed several known dust events and did not find significant misclassification of dust aerosols as clouds, so we do not believe aerosol-cloud identification errors to be the primary reason for the results observed here.

[20] The appearance of the first indirect effect between June and August corresponds well with the increase in the maritime component of AOT as defined by GOCART (Figures 2b and 3b). Given the hygroscopic nature of sea salt, an increase in its concentration is likely to increase CCN, enhancing the first indirect effect. The increase in sea salt is consistent with increasing wind speeds associated with the Indian monsoon. This, coupled with greater atmospheric moisture and average updraft velocities, allows the first indirect effect to be more evident in the Arabian Sea during the summer months. This does not take into account the increase in mineral dust concentration that also occurs during this period. Dust aerosols are not generally considered hygroscopic and as such are not generally considered good sources of CCN. Recall that dust aerosols are transported into the Arabian Sea and combine with anthropogenic sulfates already present to form the total aerosol concentration [e.g., *Ramana and Ramanathan*, 2006]. It is possible that dust aerosols become coated with sulfate material, which is hygroscopic, thus transforming the dust into excellent CCN [*Parungo et al.*, 1992]. Sulfate coated dust aerosols have been observed in the Mediterranean Sea, where both large amounts of dust and sulfate aerosols are present during certain times of the year [*Levin et al.*, 1996]. Since similar conditions also exist in the Arabian Sea during the summer months, the presence of sulfate coated dust aerosols here too is quite likely. GOCART output supports this hypothesis indicating non-trivial amounts of both aerosol types (Figure 2b). However, without in situ observations, the exact effect of dust aerosols in indirect effects in the Arabian Sea cannot be determined with a high degree of certainty.

[21] During both January and July, the relationship between AOT and LWP is positive, though the correlation is again maximized between June and August (Figures 3b, 5a and 5c). The larger aerosol concentrations present during the summer months may also enhance the second indirect effect as well. As AOT increases, CCN may also increase, reducing droplet size that in turn can increase the time required for the collision and coalescence process to pro-

duce precipitation. As a result, water vapor is trapped within clouds longer, leading to an overall increase in their size. Also of interest is that the slope of the summer time LWP- R_c relationships are generally steeper for most cloud optical thickness bins when compared to January values (Figure 5b and 5d). This is consistent with the increase in total AOT in July, which being positively correlated with LWP, would lead to larger LWP values for a given R_c and cloud optical thickness values. It is also possible that the slightly larger concentration of BC aerosols observed in January is reducing the effectiveness of the second indirect effect, though it still remains clearly positive. However, we currently do not have the necessary data to test this hypothesis.

3.4. Comparison With Other Regions

[22] To compare the indirect effects observed in the Arabian Sea with that from other regions, we performed the same analysis for a pristine region in the south Indian Ocean (SIO: $20-10^\circ\text{S}$, $70-80^\circ\text{E}$) and a heavily polluted region in the Bay of Bengal (BB: $9-19^\circ\text{N}$, $85-95^\circ\text{E}$). In the pristine region, AOT is generally low (<0.4) and comprised mainly of maritime sea salt. For both January and July, a weak negative correlation exists between AOT and cloud droplet radius, indicating the presence of the first indirect effect (Figure 6a and 6b). The presence of the first indirect effect when sea salt comprises a major portion of the total AOT for this region is consistent with the summer results for the Arabian Sea, whereby the first indirect effect was only observed with large concentrations of sea salt were present. The Bay of Bengal remains heavily polluted throughout the year, with dust and sea salt concentrations never reaching the levels observed in the Arabian Sea. Since aerosol properties in the Bay of Bengal year-round are similar to those in the Arabian Sea during the winter months, similar aerosol, cloud property relationships were expected. Figures 6c and 6d indeed show this is the case with an overall positive correlation between AOT and cloud droplet radius for both January and especially July. The South Indian Ocean and Bay of Bengal represent aerosol regimes where sea salt (SIO) and anthropogenic aerosols (BB) are the dominant aerosol types. The changes in the indirect effects observed in the Arabian Sea correspond well with the differences observed between the separate aerosol regimes.

4. Discussion

[23] Averaged over the entire year, the correlation between MODIS AOT and cloud droplet size is essentially zero in the Arabian Sea, consistent with a satellite-based analysis conducted by *Matsui et al.* [2006]. However, the analysis presented here provides strong evidence for the presence of the indirect effect in the Arabian Sea, under certain aerosol and atmospheric conditions. We have shown that the first indirect effect in particular varies substantially as a function of changing aerosol types and meteorological conditions in the Arabian Sea. Under conditions of low, primarily anthropogenic, aerosol concentrations little evidence for the first indirect effect was found. The combination of low aerosol concentrations coupled with low atmospheric water vapor concentrations may be preventing aerosols from being activated into CCN. This changes when

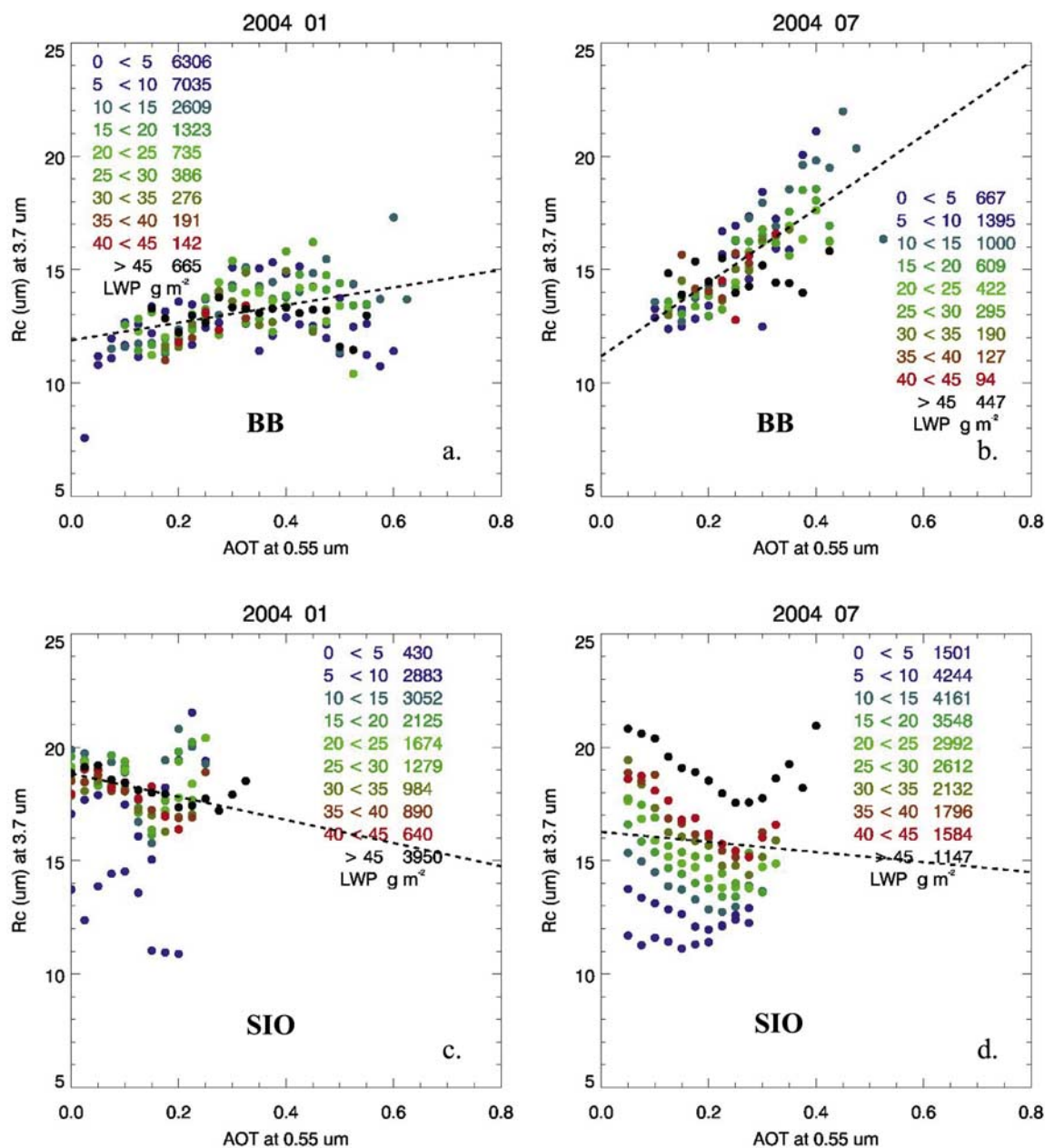


Figure 6. Scatterplot of MODIS AOT versus cloud droplet effective radius (R_c) for the South Indian Ocean (SIO: a, b) and Bay of Bengal (BB: c, d) regions for January and July 2004.

the aerosol and moisture concentrations increase substantially as does overall updraft velocity during the summer months with AOT and R_c now having the expected inverse relationship (Figure 1b). It is the addition of maritime sea salt resulting from the Monsoon that is likely associated with the strengthening of the first indirect effect. However, it is possible dust aerosols being coating with sulfates already present in the region, which would also make them excellent CCN, are also partially responsible. Evidence for the second indirect effect is also strong as it was observed during both seasons, though like the first indirect effect, it appeared to be stronger during the summer months.

[24] Preliminary analysis of other regions indicates that the first indirect effect is more evident on a year-round basis only 10 degrees south of the region presented here, which is consistent with observations by *Chylek et al.* [2006] and *Matsui et al.* [2006]. Conversely, the positive relationships between AOT and cloud droplet radius that was present in the Arabian Sea during the winter months was also present in the Bay of Bengal throughout the year, when both have high concentrations of anthropogenic aerosols. This reinforces the notion that indirect effects are highly dependent on the local aerosol and meteorological conditions present. Improved and higher resolution observations and modeling of aerosol speciation would add further insight into the

effect of aerosols on clouds. Improved understanding of this variability is necessary to reduce the large uncertainties present in estimating indirect radiative effect since this research clearly demonstrates the effect of changing aerosol characteristics on the indirect effect. Future research will expand this analysis to many different regions, with different aerosol and meteorological conditions to examine the variation of the indirect effects as a function of these parameters.

[25] **Acknowledgments.** This research is supported by NASA's Radiation sciences, Interdisciplinary sciences, an EOS grant, and ACMAP programs. The CERES SSF data that contains the merged MODIS and CERES was obtained through the NASA Langley Distributed Active Archive Systems. Special thanks to Mian Chin for providing the GOCART results.

References

- Ackerman, A. S., O. B. Toon, D. E. Stevens, and J. A. Coakley Jr. (2003), Enhancement of cloud cover and suppression of nocturnal drizzle in stratocumulus polluted by haze, *Geophys. Res. Lett.*, *30*(7), 1381, doi:10.1029/2002GL016634.
- Albrecht, B. (1989), Aerosols, cloud microphysics, and fractional cloudiness, *Science*, *245*, 1227–1230.
- Avey, L., T. J. Garrett, and A. Stohl (2007), Evaluation of the aerosol indirect effect using satellite, tracer transport model, and aircraft data from the International Consortium for Atmospheric Research on Transport and Transformation, *J. Geophys. Res.*, *112*, D10S33, doi:10.1029/2006JD007581.
- Bellouin, N., O. Boucher, J. Haywood, and M. S. Reddy (2005), Global estimate of aerosol direct radiative forcing from satellite measurements, *Nature*, *438*, 1138–1141, doi:10.1038/nature04348.
- Bennartz, R. (2007), Global assessment of marine boundary layer cloud droplet number concentration from satellite, *J. Geophys. Res.*, *112*, D02201, doi:10.1029/2006JD007547.
- Brenguier, J.-L., H. Pawlowska, and L. Schüller (2003), Cloud microphysical and radiative properties for parameterization and satellite monitoring of the indirect effect of aerosol on climate, *J. Geophys. Res.*, *108*(D15), 8632, doi:10.1029/2002JD002682.
- Brennan, J. I., Y. J. Kaufman, I. Koren, and R. R. Li (2006), Aerosol-cloud interaction – Misclassification of MODIS clouds in heavy aerosol, *IEEE Trans. Geod. Remote Sens.*, *43*, 911–915.
- Chin, M. (2002), Aerosol distributions and radiative properties simulated in the GOCART model and comparisons with observations, *J. Atmos. Sci.*, *59*, 461–483.
- Chin, M., et al. (2004), Aerosol distribution in the Northern Hemisphere during ACE-Asia: Results from global model, satellite observations, and Sun photometer measurements, *J. Geophys. Res.*, *109*, D23S90, doi:10.1029/2004JD004829.
- Christopher, S. A., and J. Zhang (2004), Cloud-free shortwave aerosol radiative effect over oceans: Strategies for identifying anthropogenic forcing from Terra satellite measurements, *Geophys. Res. Lett.*, *31*, L18101, doi:10.1029/2004GL020510.
- Chylek, P., M. K. Dubey, U. Lohmann, V. Ramanathan, Y. J. Kaufman, G. Lesins, J. Hudson, G. Altmann, and S. C. Olsen (2006), Aerosol indirect effect over the Indian Ocean, *Geophys. Res. Lett.*, *33*, L06806, doi:10.1029/2005GL025397.
- Colón-Robles, M., R. M. Rauber, and J. B. Jensen (2006), Influence of low-level wind speed on droplet spectra near cloud base in trade wind cumulus, *Geophys. Res. Lett.*, *33*, L20814, doi:10.1029/2006GL027487.
- Feingold, G. (2003), Modeling of the first indirect effect: Analysis of measurement requirements, *Geophys. Res. Lett.*, *30*(19), 1997, doi:10.1029/2003GL017967.
- Feingold, G., W. L. Eberhard, D. E. Veron, and M. Previdi (2003), First measurements of the Twomey indirect effect using ground-based remote sensors, *Geophys. Res. Lett.*, *30*(6), 1287, doi:10.1029/2002GL016633.
- Greenwald, T. J., and S. A. Christopher (2000), The GOES-IM imagers: New tools for studying the microphysical properties of boundary layers clouds, *Bull. Am. Meteorol. Soc.*, *81*, 2607–2620.
- Han, Q. Y., W. B. Rossow, and A. A. Lacis (1994), Near-global survey of effective droplet radii in liquid water clouds using ISCCP data, *J. Clim.*, *7*, 465–497.
- Han, Q., W. B. Rossow, J. Chou, and R. M. Welch (1998), Global survey of the relationships of cloud albedo and liquid water path with droplet size using ISCCP, *J. Clim.*, *11*, 1516–1528.
- Heintzenberg, J., et al. (1997), Measurements and modeling of aerosol single-scattering albedo: Progress, problems, and prospects, *Contrib. Atmos. Phys.*, *70*, 249–263.
- Jones, A., D. L. Roberts, and A. Slingo (1994), A climate model study of indirect radiative forcing by anthropogenic sulphate aerosols, *Nature*, *370*, 450–453.
- Kalnay, E., et al. (1996), The NCEP/NCAR 40-year reanalysis project, *Bull. Am. Meteorol. Soc.*, *77*, 437–471.
- Kaufman, Y. J., and R. S. Fraser (1997), The effect of smoke particles on clouds and climate forcing, *Science*, *277*, 1636–1639.
- Kaufman, Y. J., I. Koren, L. A. Remer, D. Tanré, P. Ginoux, and S. Fan (2005), Dust transport and deposition observed from the Terra-Moderate Resolution Imaging Spectroradiometer (MODIS) spacecraft over the Atlantic Ocean, *J. Geophys. Res.*, *110*, D10S12, doi:10.1029/2003JD004436.
- Li, S.-M., C. M. Banic, W. R. Leitch, P. S. K. Liu, G. A. Isaac, X.-L. Zhou, and Y.-N. Lee (1996), Water-soluble fractions of aerosol and their relations to number size distributions based on aircraft measurements from the North Atlantic Regional Experiment, *J. Geophys. Res.*, *101*(D22), 29,111–29,121.
- Levin, Z., E. Ganor, and V. Gladstein (1996), The effects of desert particles coated with sulfate on rain formation in the eastern Mediterranean, *J. Appl. Meteorol.*, *35*, 1511–1523.
- Lohmann, U., and J. Feichter (2005), Global indirect aerosol effects: A review, *Atmos. Chem. Phys.*, *5*, 715–737.
- Lohmann, U., and G. Lesins (2003), Comparing continental and oceanic cloud susceptibilities to aerosols, *Geophys. Res. Lett.*, *30*(15), 1791, doi:10.1029/2003GL017828.
- Lohmann, U., G. Tselioudis, and C. Tyler (2000), Why is the cloud albedo–particle size relationship different in optically thick and optically thin clouds?, *Geophys. Res. Lett.*, *27*(8), 1099–1102.
- Matsui, T., H. Masunaga, S. M. Kreidenweis, R. A. Pielke Sr., W.-K. Tao, M. Chin, and Y. J. Kaufman (2006), Satellite-based assessment of marine low cloud variability associated with aerosol, atmospheric stability, and the diurnal cycle, *J. Geophys. Res.*, *111*, D17204, doi:10.1029/2005JD006097.
- Minnis, P., D. F. Young, S. Sun-Mack, P. W. Heck, D. R. Doelling, and Q. Trepte (2003), CERES Cloud Property Retrievals from Imagers on TRMM, Terra, and Aqua, *Proc. SPIE 10th International Symposium on Remote Sensing: Conference on Remote Sensing of Clouds and the Atmosphere VII*, Barcelona, Spain, 8–12 September, 37–48.
- Nakajima, T., and M. D. King (1990), Determination of the optical thickness and effective particle radius of clouds from reflected solar radiation measurements. Part I: Theory, *J. Atmos. Sci.*, *47*, 1878–1893.
- Nakajima, T., M. D. King, and J. D. Spinhirne (1991), Determination of the optical thickness and effective particle radius of clouds from reflected solar radiation measurements. Part II: Marine strato-cumulus observations, *J. Atmos. Sci.*, *48*, 728–750.
- Parungo, F., B. Kopcewicz, C. Nagamoto, R. Schnell, P. Sheridan, C. Zhu, and J. Harris (1992), Aerosol particles in the Kuwait oil fire plumes: Their morphology, size distribution, chemical composition, transport, and potential effect on climate, *J. Geophys. Res.*, *97*(D14), 15,867–15,882.
- Peng, Y., U. Lohmann, R. Leitch, C. Banic, and M. Couture (2002), The cloud albedo-cloud droplet effective radius relationship for clean and polluted clouds from RACE and FIRE ACE, *J. Geophys. Res.*, *107*(D11), 4106, doi:10.1029/2000JD000281.
- Penner, J. E., X. Dong, and Y. Chen (2004), Observational evidence of a change in radiative forcing due to the indirect aerosol effect, *Nature*, *427*, 231–234.
- Quaas, J., O. Boucher, and F. Bréon (2004), Aerosol indirect effects in POLDER satellite data and the Laboratoire de Météorologie Dynamique–Zoom (LMDZ) general circulation model, *J. Geophys. Res.*, *109*, D08205, doi:10.1029/2003JD004317.
- Quinn, P. K., D. J. Coffman, T. S. Bates, T. L. Miller, J. E. Johnson, E. J. Welton, C. Neusüss, M. Miller, and P. J. Sheridan (2002), Aerosol optical properties during INDOEX 1999: Means, variability, and controlling factors, *J. Geophys. Res.*, *107*(D19), 8020, doi:10.1029/2000JD000037.
- Ramana, M. V., and V. Ramanathan (2006), Abrupt transition from natural to anthropogenic aerosol radiative forcing: Observations at the ABC-Maldives Climate Observatory, *J. Geophys. Res.*, *111*, D20207, doi:10.1029/2006JD007063.
- Ramanathan, V., et al. (2001), Indian Ocean Experiment: An integrated analysis of the climate forcing and effects of the great Indo-Asian haze, *J. Geophys. Res.*, *106*(D22), 28,371–28,398.
- Ramanathan, V., et al. (2007), Atmospheric brown clouds: Hemispherical and regional variations in long-range transport, absorption, and radiative forcing, *J. Geophys. Res.*, *112*, D22S21, doi:10.1029/2006JD008124.
- Reid, J. S., T. F. Eck, S. A. Christopher, P. V. Hobbs, and B. N. Holben (1999), Use of the Ångström exponent to estimate the variability

- of optical and physical properties of aging smoke particles in Brazil, *J. Geophys. Res.*, *104*(D22), 27,473–27,489.
- Remer, L. A., and Y. J. Kaufman (2005), Aerosol effect on the distribution of solar radiation over the clear-sky global oceans derived from four years of MODIS retrievals, *Atmos. Chem. Phys. Discuss.*, *5*, 5007–5038.
- Schwarz, S. E., Harshvardhan, and C. M. Benkovitz (2002), Influence of anthropogenic aerosol on cloud optical depth and albedo shown by satellite measurements and chemical transport modeling, *Proc. Natl. Acad. Sci. USA*, *99*, 1784–1789.
- Twomey, S. A. (1977), The influence of pollution on the shortwave albedo of clouds, *J. Atmos. Sci.*, *34*, 1149–1152.
- Wood, R., and D. L. Hartmann (2006), Spatial variability of liquid water path in marine low clouds: Part 1. Probability distribution and mesoscale cellular scales, *J. Clim.*, *19*, 1748–1764.
- Yuan, T.m., Z. Li, F. L. Chang, B. Vant-Hull, and D. Rosenfeld (2007), Increase of cloud droplet size with aerosol optical depth: a likely new effect of aerosols on climate, *12th Conference on Cloud Physics*, Madison, WI.
-
- S. A. Christopher and T. A. Jones, Department of Atmospheric Science, The University of Alabama in Huntsville, 320 Sparkman Drive, Huntsville, AL 35806-1912, USA. (tjones@nsstc.uah.edu)